Medical Physics
The International Journal of Medical Physics Research and Practice

Changes in optically stimulated luminescent dosimeter (OSLD) dosimetric characteristics with accumulated dose

Paul A. Jursinic

Citation: Medical Physics **37**, 132 (2010); doi: 10.1118/1.3267489
View online: http://dx.doi.org/10.1118/1.3267489
View Table of Contents: http://scitation.aip.org/content/aapm/journal/medphys/37/1?ver=pdfcov
Published by the American Association of Physicists in Medicine

Changes in optically stimulated luminescent dosimeter (OSLD) dosimetric characteristics with accumulated dose

Paul A. Jursinic[a)]
West Michigan Cancer Center, 200 North Park St., Kalamazoo, Michigan 49007

(Received 22 July 2009; revised 28 October 2009; accepted for publication 4 November 2009; published 4 December 2009)

Purpose: A new type of *in vivo* dosimeter, an optically stimulated luminescent dosimeter (OSLD), has now become commercially available for clinical use. The OSLD is a plastic disk infused with aluminum oxide doped with carbon (Al_2O_3:C). Crystals of Al_2O_3:C, when exposed to ionizing radiation, store energy that is released as luminescence (420 nm) when the OSLD is illuminated with stimulation light (540 nm). The intensity of the luminescence depends on the dose absorbed by the OSLD and the intensity of the stimulation light. The effects of accumulated dose on OSLD response were investigated.

Methods: The OSLDs used in this work were nanodot dosimeters, which were read with a MicroStar reader (Landauer, Inc., Glenwood, IL). Dose to the OSLDs was delivered by 6 MV x rays and gamma rays from Co-60 and Ir-192. The signal on the OSLDs after irradiation is removed by optical annealing with a 150 W tungsten-halogen lamp or a 14 W compact fluorescent lamp was investigated.

Results: It was found that OSLD response to dose was supralinear and this response was altered with the amount of accumulated dose to the OSLD. The OSLD response can be modeled by a quadratic and an exponential equation. For accumulated doses up to 60 Gy, the OSLD sensitivity (counts/dose) decreases and the extent of supralinear increases. Above 60 Gy of accumulated dose the sensitivity increases and the extent of supralinearity decreases or reaches a plateau, depending on how the OSLDs were optically annealed. With preirradiation of OSLDs with greater than 1 kGy, it is found that the sensitivity reaches a plateau 2.5 folds greater than that of an OSLD with no accumulated dose and the supralinearity disappears. A regeneration of the luminescence signal in the dark after full optical annealing occurs with a half time of about two days. The extent of this regeneration signal depends on the amount of accumulated dose.

Conclusions: For *in vivo* dosimetric measurements, a precision of ±0.5% can be achieved if the sensitivity and extent of supralinearity is established for each OSLD and use. Methods are presented for accomplishing this task.
[DOI: 10.1118/1.3267489]

Key words: optically stimulated luminescent dosimeters, *in vivo* dosimetry, thermoluminescent dosimeters, diodes

I. INTRODUCTION

Cancer patients that undergo radiation treatments require the delivery of high dose, usually 180 cGy or more per day, for 30–40 consecutive daily treatments. *In vivo* dosimetry is desired for cancer patients to ensure that the patient is not overexposed or that the exposure occurs in the desired region.[1,2] To make *in vivo* measurements one needs devices that are small in size and robust. A wide variety of devices have been used to accomplish this task such as thermoluminescent dosimeters[3] (TLDs), *PN* junction type diodes,[4,5] or MOSFET detectors.[5]

In the past 20 years, synthetic materials have been developed that have the property of thermally and optically stimulated luminescence.[6,7] Man made sapphire, Al_2O_3:C, had favorable characteristics: 30–60 times the sensitivity to radiation as LiF:Mg,Ti TLDs,[8] low levels of signal fading,[9–13] and a relatively low atomic number[8] of 11.28. It was quickly realized that optical discharging gave rise to OSL that was proportional to the dose of ionizing radiation absorbed by the Al_2O_3:C crystal.[7,14–18]

Optically stimulated luminescent dosimeters[14] (OSLDs) made of Al_2O_3:C can be stimulated with a broad spectrum of light from 400 to 700 nm with a peak at 475 nm.[17,18] The emission occurs in a broad band of wavelengths with a peak centered at 410–420 nm.[14,17] The OSLD can be read out with light in continuous wave (cw) mode[12,13,19,20] or with the light in pulsed mode.[16,18,21,22] In the cw mode, the stimulation light and the detector are on continually and narrow band optical filters are used to discriminate between the stimulation and emission light. In the pulsed mode, the stimulation light and detector are only active for short periods of time that are asynchronous, so separation of light signals is accomplished temporally.

A number of papers have been published recently that describe the use of OSLDs in radiation oncology clinical measurements.[11–13,23,24] In these works there are two mea-

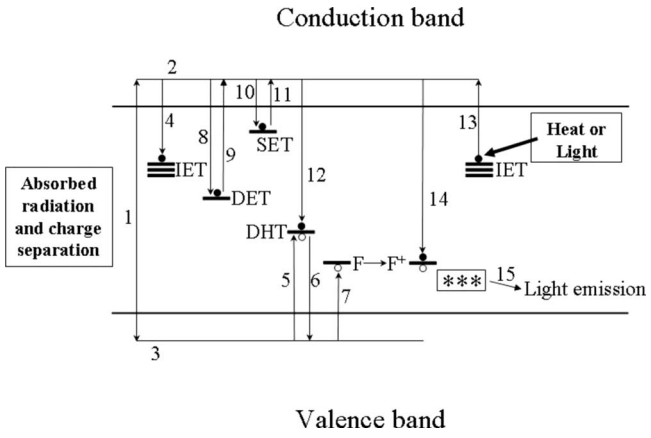

FIG. 1. A diagram of the energy levels of a crystalline material that sustains thermoluminescence or optical luminescence. The numbers in the diagram represent charge flow reactions that are described in the text. SET, IET, and DET are electron traps of progressively deeper depth. DHT and F are hole (○) traps with F^+ being a luminescence center, which received energy from the recombination of the electron (●) and hole.

surement techniques that have been invoked. The first measurement mode, integrating mode,[25] is to expose the OSL dosimeter in a radiation field and at a later time readout the OSL signal that is proportional to the absorbed dose.[26–30] The second measurement mode, real-time mode,[28] is readout of the luminescence signal, which is called radioluminescence, during the radiation delivery.[20,27–29,31] The first method, the integrating mode, is used in this work.

It was observed in earlier works[12,13] that the characteristics of OSLDs changed with accumulated dose. This report is a detailed study of the effect of accumulated dose on response to dose of OSLDs.

II. OSLD THEORETICAL DESCRIPTION

A large number of charge transfer reactions take place in an OSLD crystal. A generalized model for the energy structure and charge movement in α-Al_2O_3:C crystals has been previously presented,[25,32–35] and is shown in Fig. 1. The reactions are shown schematically in Fig. 1.

$$\text{OSLD crystals} \xrightarrow{\text{ionizing radiation}} h^+ + e^- \quad \text{reaction 1},$$

$$\text{DHT} + h^+ \rightarrow \text{DHT}^+ \xrightarrow{550\ ^\circ\text{C}} \text{DHT} + h^+ \quad \text{reactions 3,5},$$

$$\text{DHT}^+ + e^- \rightarrow \text{DHT} + \text{heat} \quad \text{reaction 12},$$

$$F + h^+ \rightarrow F^+ \quad \text{reactions 3,7},$$

$$F^+ \xrightarrow{e^-(\text{os})} F^* \rightarrow F + \text{light(luminescence)} \quad \text{reactions 13,14,15},$$

$$\text{SET} + e^- \xrightarrow{\text{dark}} \text{SET}^- \rightarrow \text{SET} + e^- \quad \text{reactions 2,10,11},$$

$$\text{IET} + e^- \rightarrow \text{IET}^- \xrightarrow{\text{light or } 190\ ^\circ\text{C}} \text{IET} + e^-(\text{os}) \quad \text{reactions 4,13},$$

$$\text{DET} + e^- \rightarrow \text{DET}^- \xrightarrow{900\ ^\circ\text{C}} \text{DET} + e^- \quad \text{reactions 8,9},$$

where h^+ is a free hole, e^- is a free electron, DHT is a deep hole trap, F is the luminescent center, F^* is an excited state of F, e^-(os) is an optically stimulated electron, and SET, IET, and DET are shallow, intermediate, and deep electron traps, respectively.

The following charge flow reactions are occurring as shown in Fig. 1. 1 is the absorption of radiation and subsequent charge separation; 2 is the migration and trapping of an electron after charge separation; 3 is the migration and trapping of a hole after charge separation; 4 is electron capture by an IET; 5 is a hole capture by a DHT; 6 is a hole release, which only occurs at 550 °C; 7 is the capture of a hole by a F center; 8 is electron capture by a DET; 9 is an electron release, which only occurs at 900 °C; 10 is electron capture by an SET; 11 is an electron release, which occurs at room temperature in the dark and is the transient signal with a 0.8 min half-life;[12] 12 is the capture of an electron by a DHT^+, which results in heat not luminescence; 13 is the ejection of an electron out of an IET^- by absorption of heat, thermoluminescence, or light (optical luminescence); 14 is the capture of an electron by a F^+ center, which results in recombination of an electron and hole and luminescence (reaction 15).

The characteristics of charge traps in crystals of α-Al_2O_3:C have been studied[32,36] by measurements of optical absorption and phototransferred thermoluminescence and their response to heat annealing from 450 to 1350 °C. Three main charge traps are found to exist: (1) The main dosimetric electron trap, IET above, which has a delocalization temperature of 190 °C, also can be ionized by light, and is associated with intense luminescence when its electron recombines at an F^+ center; (2) a DHT, which has a delocalization temperature of 550 °C and is not luminescent; and (3) a DET, which has a delocalization temperature of 900 °C and cannot be photoionized. While the electron traps associated with optically stimulated luminescence are shown as three energy levels in Fig. 1, this is not the case. There is a large distribution of trap energies from which optically stimulated luminescence originates. The evidence for this is a broad excitation spectrum that starts in the UV and ends at about 700 nm.[17,18,37]

Increased dose causes deep electron traps to fill, which means shallower traps have a higher probability of getting filled and the decay curve becomes faster.[38,39] Also, TL peaks are shifted to a lower temperature[40,41] due to less competition for electrons because DET are filled. The fast portion of the decay, which is measured here, is from shallow IETs and is known to show enhanced supralinearity.[38]

Very high x ray dose causes all of the DHT to be filled.[32,36,42] The luminescence is diminished because DHT^+, which are not luminescent, compete with F^+, which are luminescent, for electrons liberated from the main dosimetric

trap. This work shows how high dose and optical annealing cause additional changes to the charge equilibrium in the charge traps.

III. MATERIALS AND METHODS

The x-ray beams used in this work had a nominal energy of 6 MV. The percent depth dose of x rays at depth 10 cm, $\%dd\ (10)_x$, was 66.6, which was measured at source-to-surface distance of 100 cm, according to the AAPM TG-51 protocol.[43] The x-ray beams were generated by a Varian Trilogy (Varian Medical Systems, Milpitas, CA) linear accelerator.

Absolute dose measurements were made with a cylindrical ion chamber, model N30001 (PTW, Hicksville, NY), which had been calibrated at the University of Wisconsin Dosimetry Calibration Laboratory (Madison, WI). All doses delivered by the accelerators were compared against ion chamber measurements that were traceable to AAPM TG-51 (Ref. 43) calibrations.

The OSLDs used were InLight/OSL nanodot dosimeters (Landauer, Inc., Glenwood, IL). The OSLDs are 5 mm diameter, 0.2 mm thick plastic disks infused with aluminum oxide doped with carbon (Al_2O_3:C) (synthetic sapphire). These disks are encased in a $10\times10\times2$ mm^3 light-tight plastic holder. The plastic has a mass density of 1.03 g/cm^3 and the plastic leaves that cover the front and back of the OSLD disk are 0.36 mm thick. This gives an areal density of the covering of the OSLD disk of 0.037 g/cm^2. Including repetition of experiments, about 60–70 different nanodots were used in the measurements done in this paper.

OSLDs were read with an InLight MicroStar reader (Landauer, Inc., Glenwood, IL). For reliable reading of nanodot OSLDs, the optical port of the reader was machined by the author to a larger diameter of 4.8 mm (3/16 in.). This reader operates in cw mode with a 1 s illumination read period. The reader was operated in its "hardware test" modality, using the low-intensity light emitting diodes (LED) beam for preirradiation and postirradiation measurements. The readout light is provided by a model NSPG500S LED (Nichia, Inc. Tokyo). The LED light passes through a color glass band-pass filter OG515 (Melles Griot, Rochester, NY). This LED filter combination has a peak emission at 540 nm. The OSLD signal was read directly by a photomultiplier filtered with a color glass band-pass filter B370 (Hoya, San Jose, CA). This photomultiplier filter combination has peak sensitivity at 420 nm.

The reader has low-intensity and high-intensity LED modes. The high-intensity LED mode was not used because it was found that the light signal from a nanodot irradiated with greater than 200 cGy saturated the optical detector circuits. The optical detector circuits were found to begin to saturate whenever the counts exceeded about 1.6×10^6. In the low-intensity LED mode nanodots could be exposed to approximately 15 Gy before reader saturation occurred. To accommodate an even larger dose range or OSLDs with greater sensitivity, the reader was modified by adding a filter to the optical path. A neutral density filter with a transmission of 0.0816 was fabricated from radiographic film that had been exposed to a low dose and developed. The processed film was cut into a small disk that could be easily and quickly mounted in front of the photomultiplier tube in the reader. With this modified reader, the OSLD range of dose was extended by approximately $1/0.0816=12.2$ fold to a maximum dose of 180 Gy.

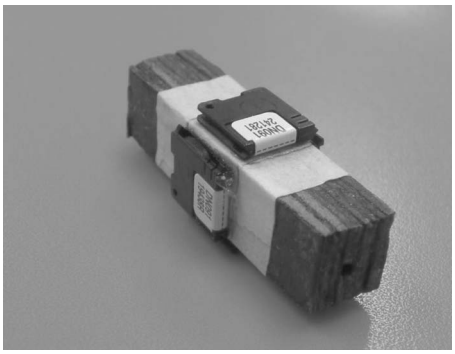

FIG. 2. Apparatus used to hold nanodots for irradiation with Ir-192. The spacer, $1\times1\times4$ cm^3, is constructed from slabs of cardboard that are glued together. A hole is bored in the center of the cardboard block to hold the HDR catheter. The nanodots are fastened in position as shown with double-sided adhesive tape.

After irradiation OSLDs have a transient signal that decays with a half-life of 0.8 min.[12] To avoid this transient signal, OSLDs were kept in the dark for approximately 8 min before they were read. All OSLDs were read prior to irradiation and reported signals were the difference between the postirradiation and preirradiation signal reported in photomultiplier counts.

Irradiations of the nanodots were done orthogonal to the front surface with a source-to-detector distance of 100 cm. A 0.5 cm thick piece of Superflab was placed immediately over the detector, which conformed to the irregular shapes of the detector without large air gaps. An 8 cm thick block of solid water was placed behind the detectors to provide back scatter of radiation.

Some OSLDs were irradiated to an accumulated dose above 1 kGy. This was done with a Co-60 machine or with a HDR, Ir-192 source. For the HDR source, the dose rate at the detector position was calculated using the AAPM TG-43 protocol.[44] The air kerma strength of the source was measured with a model HDR100Plus well chamber (Standard Imaging, Middleton, WI) that had been calibrated at a University of Wisconsin Dosimetry Calibration Laboratory. Figure 2 is a photograph of the apparatus used for the irradiation with Ir-192. The spacer holds up to four nanodots centered, at a distance of 5 mm, over the dwell position in the catheter. A 3 cm thick wrap of Superflab is made over the OSLDs to provide backscatter. With 5 mm spacing the dose gradient is very high and the precise dose at the position of the OSLDs cannot be known. However, high precision in this irradiation of greater than 1 kGy is not required since it is used for the purpose of preirradiation not dosimeter calibration.

Two different light sources were used to bleach (optically anneal) the irradiated OSLDs after they had been read. The

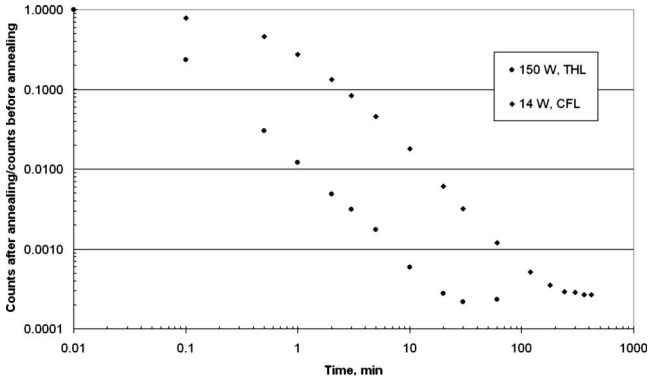

FIG. 3. Measurements of an OSLD signal after various times of optical annealing. For an irradiation of 180 cGy the signal size before annealing was approximately 170 000 counts. The OSLDs were irradiated and then optically annealed for the indicated times with a THL or CFL.

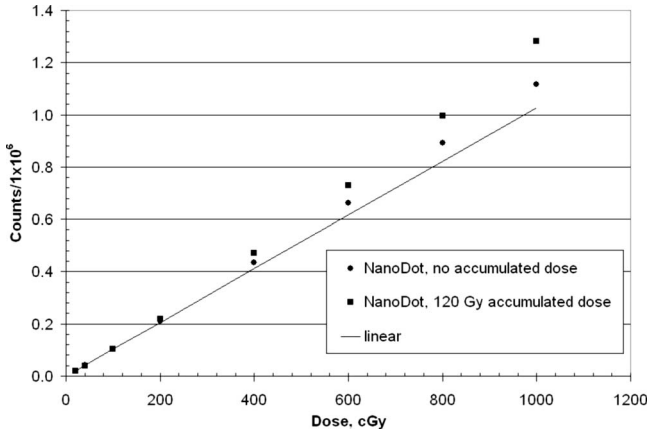

FIG. 4. OSLD response versus absorbed dose. For each dose point the nanodot is irradiated, kept in the dark for 8 min, and then read. The solid line shows linear dependence on dose based on the response of the OSLD up to 20 cGy.

first type of light was an endoscopic illuminator, model 481C, miniature cold light fountain (Karl Storz, Los Angeles, CA) was used. This illuminator had a 150 W tungsten-halogen lamp (THL) model EJA (Osram Sylvania, Danvers, MA) focused onto an optical port. This THL has a color temperature of 3400 K. A 4 mm diameter, 30 cm long light guide was attached to the optical port. The light guide focused the light and acted as a heat shield to avoid melting the plastic housing of the OSLD. A plastic fitting was machined that firmly held the OSLD with its case opened at the end of the light guide. The second type of light was a bright white, 14 W compact fluorescent lamp (CFL) model 5M814435K (n:vision, Atlanta, GA), which was mounted in a reflective housing. This CFL has a color temperature of 3500 K. OSLDs were bleached for various lengths of time. After bleaching the OSLD signal was measured to determine what level of residual signal remained.

IV. RESULTS

As previously shown,[12] OSLDs can be repeatedly used if they are optically annealed between uses. Two different nanodots were irradiated with 180 cGy of 6 MV x rays and were kept in the dark for 10 min before reading. The OSLDs were then illuminated with two different light sources for different amounts of time, followed by 3 min of dark before they were read. The dark interval after illumination was needed to avoid interference from phosphorescence of the OSLD. As can be seen in Fig. 3, the THL anneals the OSLD about ten times more rapidly than the CFL. Also, 99% of the signal is removed in 1 min with the THL and in 10 min with the CFL. To remove the remaining 1% of the signal requires a 60 fold greater amount of time. Regardless of which annealing light is used, a plateau in the extent of annealing is reached at a signal size of approximately 50 counts, which is a ratio of 3×10^{-4} for the data in Fig. 3 and equivalent to 0.05 cGy. A new, never irradiated nanodot has a signal of five to ten counts, which is equivalent to 0.005 cGy. So, optical annealing is unable to completely remove the signal generated by irradiation.

The OSLD response to absorbed dose is shown in Fig. 4. As can be seen, the OSLDs behave like TLDs[3] and exhibit supralinear response to dose above 300 cGy. The OSLD supralinear response has been reported previously.[12,32,38,42] A new phenomenon is observed in Fig. 4; the extent of supralinearity is enhanced when the OSLD has a greater amount of accumulated dose.

To emphasize the supralinear behavior, counts/dose is plotted in Fig. 5. Obviously the OSLD response to dose is not linear but it is found to be well described by the following exponential equation:

$$\text{Counts} = A \times \text{dose} \times (1 + B \times (1 - \exp(-C \times \text{dose}))), \quad (1)$$

where A, B, and C are determined parameters. The measured data are fit using the solver function in Microsoft Excel, which is a nonlinear regression, steepest descent method. For

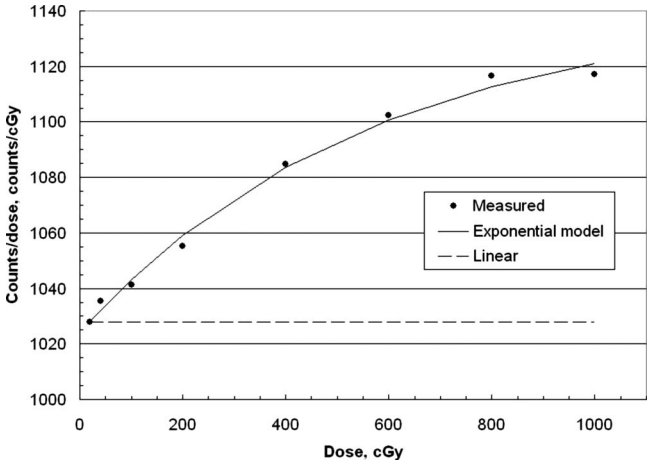

FIG. 5. OSLD response versus absorbed dose. For each dose point the nanodot is irradiated, kept in the dark for 8 min, and then read. The solid line is calculated based on Eq. (1), using the following parameters: $A=1024$ counts/cGy, $B=0.113$, and $C=1.79\times10^{-3}$ cGy^{-1}. The broken line (linear response) is based on the response of the OSLD at 20 cGy.

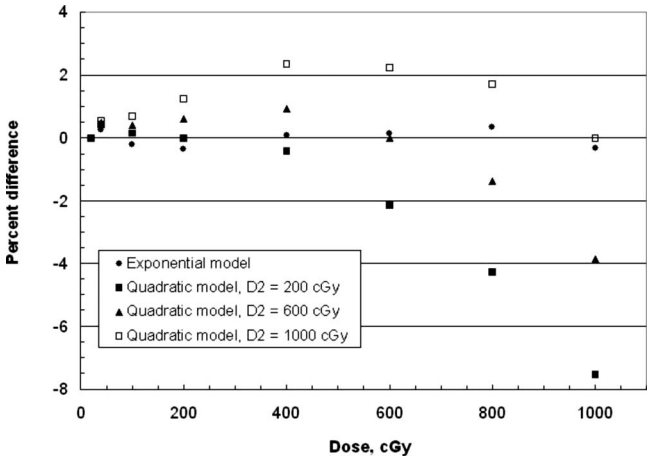

FIG. 6. Percent difference between the calculated dose and the dose delivered to a nanodot; percent difference = 100 × (cal-del)/del. The dose was calculated with the exponential model [Eq. (1)] and the quadratic model [Eq. (2)]. For the exponential model: $A=1024$ counts/cGy, $B=0.113$, and $C=0.001\,79$ cGy^{-1}. For the quadratic model: With D2=200 cGy, $a=9.755\times10^{-4}$ counts^{-1}, $b=-1.325\times10^{-10}$; with D2=600 cGy, $a=9.749\times10^{-4}$ counts^{-1}, $b=-1.025\times10^{-10}$; with D2=1000 cGy, $a=9.743\times10^{-4}$ counts^{-1}, $b=-7.091\times10^{-11}$.

the data in Fig. 5, eight dose points were used in the regression fit. As few as three well-separated dose points could be used with a drop in the precision of the fitted parameters. The parenthetical expression in Eq. (1) is a description of the magnitude of supralinearity, which is approximately equal to 1 at low dose and to $(1+B)$ at high dose.

Equation (1) is a useful characterization of the response of OSLDs to dose. Unfortunately, Eq. (1) is transcendental and cannot be solved for dose in closed form. However, when a nanodot is exposed to radiation, the signal is read, and through the use of Eq. (1) the dose can be calculated with Excel solver[45] if the variables A, B, and C are known.

Besides the exponential model of Eq. (1), dose can also be calculated with the following quadratic equation:[12]

$$\text{Dose} = a \times \text{counts} + b \times \text{counts}^2, \tag{2}$$

where a and b are determined parameters. Solving Eq. (2) for two doses, D1 and D2, the following equations are obtained:

$$a = \frac{\text{D1} - \text{D2} \times \left(\frac{\text{CNTD1}}{\text{CNTD2}}\right)^2}{\left(\text{CNTD1} - \frac{\text{CNTD1}^2}{\text{CNTD2}}\right)}, \tag{3}$$

$$b = \frac{\text{D1} - a \times \text{CNTD1}}{(\text{CNTD1}^2)}, \tag{4}$$

where CNTD1 and CNTD2 are the counts that are read on the OSLD when exposed to doses D1 and D2, respectively. When doing this type of two-dose characterization, doses of 20 and 200 cGy are found to be convenient for making measurements in the 0–400 cGy range.

Figure 6 shows the results of the exponential and quadratic models applied to the same nanodot. The exponential model parameters were determined from three dose points: 20, 600, and 1000 cGy. The quadratic model parameters were determined from two dose points: D1=20 cGy and D2=200, 600, or 1000 cGy. After these irradiations for the characterization of the nanodot, the device was optically annealed with the CFL for 3 h. The nanodot was then irradiated with eight doses from 20 to 1000 cGy, the signal counts were read, and the dose calculated by both models. As can be seen in Fig. 6, the exponential model was accurate to within 0.4% from 0 to 1000 cGy of delivered dose. The quadratic model both over and under estimated the delivered dose when below and above the D2 value. The quadratic model is quite useful over a range of dose near the D2 calibration dose. The exponential model is significantly better than the quadratic model when a large range of dose is received by the OSLD.

TABLE I. Characteristics of 17 nanodots that were randomly chosen from a new batch of devices. The dosimeters were all irradiated with 6 MV x rays. Parameters are for Eq. (1).

Parameter	A (counts/cGy)	B	C (cGy^{-1})
Minimum	908	0.051	0.000 89
Maximum	1054	0.204	0.0018
Average	958.5	0.111	0.0015
Coefficient of variation	5.1%	27.7%	30.5%

It is of interest to know how variable the characteristics of OSLDs are if they have no accumulated dose. Seventeen new nanodots were chosen at random from a batch obtained from the manufacturer. These devices were not preselected in any way. These nanodots were characterized using the nonlinear regression method described for Fig. 5 and statistics of their characterization parameters are shown in Table I. Using these parameters in Eq. (1) and a typical signal of 200 000 counts, the average dose is calculated to be 202.9 cGy with a range of 179.7–218.3, which is 202.9 cGy+11% to −8%. Clearly, without any preselection, one must characterize nanodots before they are used for dosimetry.

OSLDs can be used with the following procedure: Optically bleached, irradiated, and read. This cycle can be repeated many times. This type of repeated measurement was carried out and the sensitivity of the OSLD was measured. These nanodots were characterized using the nonlinear regression method described for Fig. 5. Figures 7–10 show how the parameters of Eq. (1) change with the accumulated dose to the OSLD when it passes through many cycles of irradiation, read, and optical bleach. The A parameter (Fig. 7), which is the OSLD sensitivity before supralinearity occurs, decreases up to an accumulated dose of 60 Gy. Note that for the OSLD annealed with the THL, the decrease in A begins at 20 Gy, a behavior that was reported previously.[12] Also, at an accumulated dose of zero, the two OSLDs have different values for A, which is variability between the devices. Above 60 Gy, A rapidly increases if the CFL is used for annealing and slowly increase if the THL is used.

The B parameter (Fig. 8), which is the magnitude of the supralinearity, increases up to an accumulated dose of 60 Gy.

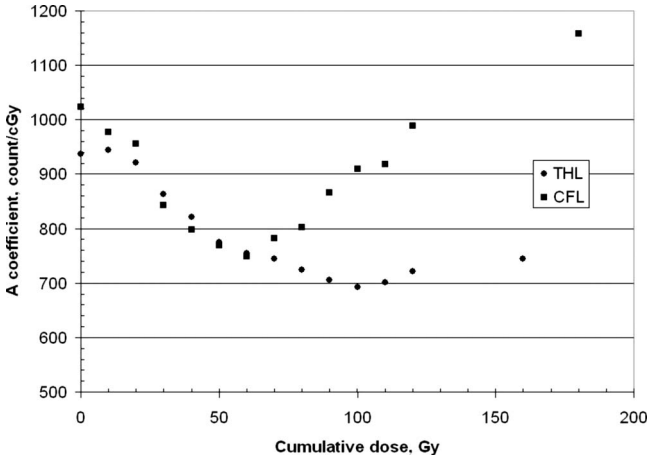

FIG. 7. The change in parameter A of Eq. (1) as a function of the accumulated dose to the nanodot. For each dose point the nanodot is irradiated, kept in the dark for 8 min, and then read. After 1000 cGy was delivered the nanodot was optical annealed to the plateau value shown in Fig. 3. Two different nanodots were used. One was optically annealed with the THL and the other with the CFL.

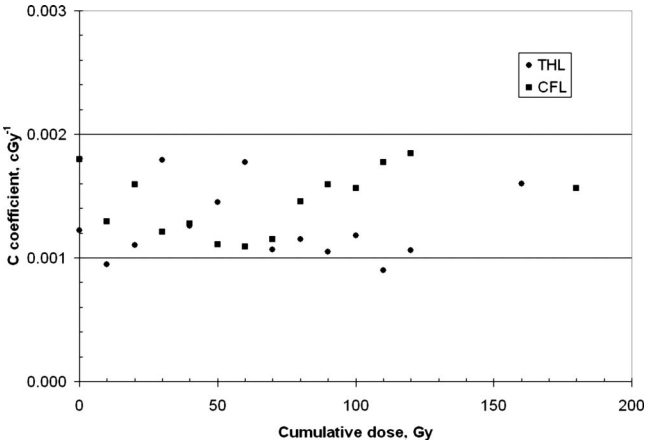

FIG. 9. The change in parameter C of Eq. (1) as a function of the accumulated dose to the nanodot. Other experimental details are the same as in the legend of Fig. 7.

Above 60 Gy, B decreases if the CFL is used for annealing and continues to increase if the THL is used.

The C parameter (Fig. 9), which is the dose dependence of the supralinearity, within experimental uncertainty remains invariant at an average value of 1.5×10^{-3} cGy^{-1}.

The expression $A\cdot(1+B)$ (Fig. 10), which is the high dose limit of Eq. (1), increases with accumulated dose. The increase is more pronounced for OSLDs annealed with the CFL than with the THL.

The data in Figs. 7–10 show that the OSLD characteristics change with accumulated dose. For the data in Fig. 5 and Table I, parameters A, B, and C were solved based on eight different doses between 20 and 1000 cGy. A more practical approach with multiple uses of an OSLD is to solve for A and B in Eq. (1), with C being held constant at its initial value since it does not change with accumulated dose as shown in Fig. 9. Solving Eq. (1) for two doses D1 and D2, the following equations are obtained:

$$B=\frac{R-1}{(1-R+R\times\exp(-C\times \mathrm{D1})-\exp(-C\times \mathrm{D2}))},$$

$$\text{where } R=\frac{(\mathrm{CNTD2/D2})}{(\mathrm{CNTD1/D1})}, \tag{5}$$

$$A=\frac{(\mathrm{CNTD1/D1})}{(1+B\times(1-\exp(-C\times \mathrm{D1})))}, \tag{6}$$

where CNTD1 and CNTD2 are the counts that are read on the OSLD when exposed to doses D1 and D2, respectively. In doing this type of two-dose characterization, doses of 20 and 200 cGy are found to be convenient.

In the next set of measurements the nanodot was exposed to increasing amounts of dose and read without being optically annealed between irradiations. These nanodots were

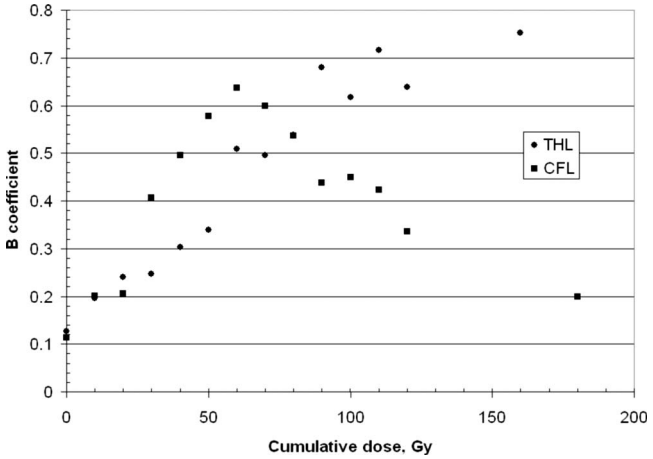

FIG. 8. The change in parameter B of Eq. (1) as a function of the accumulated dose to the nanodot. Other experimental details are the same as in the legend of Fig. 7.

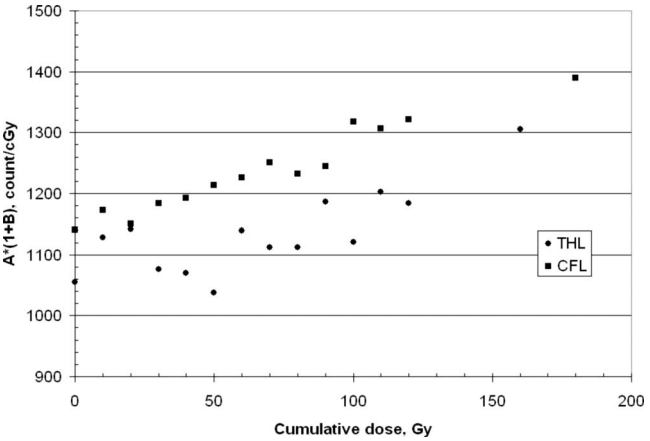

FIG. 10. The change in high dose limit value $A\cdot(1+B)$ of Eq. (1) as a function of the accumulated dose to the nanodot. Other experimental details are the same as in the legend of Fig. 7.

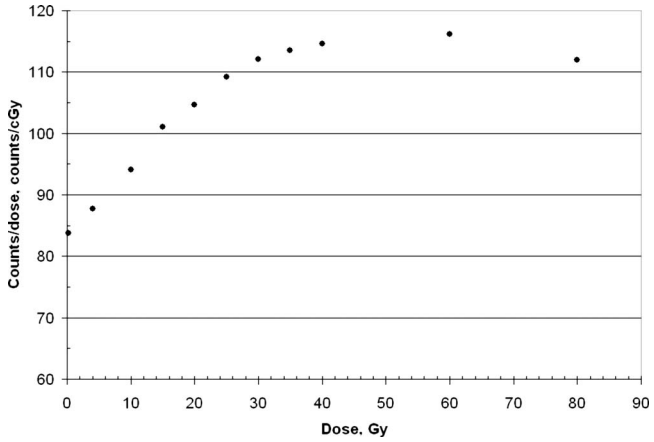

FIG. 11. OSLD response versus absorbed dose. For each dose point the nanodot is irradiated, kept in the dark for 8 min, and then read. The irradiation sequence was then repeated multiple times to give the total dose as indicated. The nanodot was not optically annealed between irradiations.

read with the film-modified reader. As can be seen in Fig. 11, the OSLD sensitivity (supralinearity) increases up to a dose of 60 Gy and then remains constant.

Based on the data shown in Figs. 7, 8, and 10, the characteristics of OSLDs vary up to a 180 Gy of accumulated dose. It was of interest to determine if the nanodots stabilized with much higher dose. To test this, nanodots were exposed to 1 and 5 kGy of dose with a Co-60 machine and 2 kGy with a HDR Ir-192 source. The response to dose of a nanodot that had been irradiated to 1 and 2 kGy is shown in Fig. 12. Compared to a nanodot with no previous irradiation in Fig. 5, there are two significant changes in the 1 and 2 kGy preirradiated nanodot: (1) The sensitivity, counts/cGy, increased by about 2.5 fold and (2) the supralinear behavior has become insignificant. Characteristics of nanodots preirradiated with high dose are given in Table II.

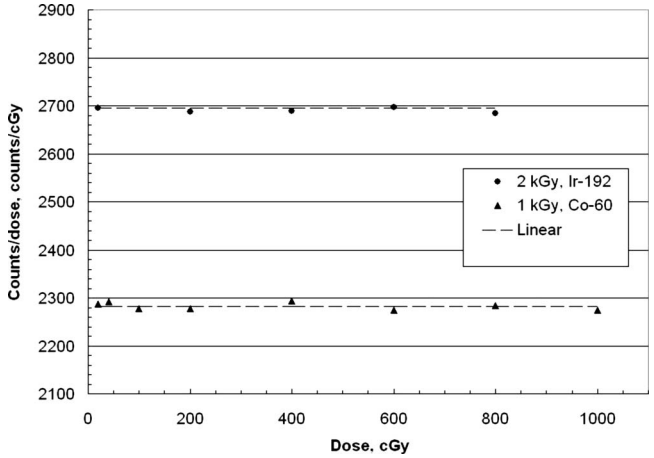

FIG. 12. OSLD response versus absorbed dose. The nanodot was irradiated with 1 kGy from Co-60 and 2 kGy from Ir-192 and then optically annealed to the plateau value shown in Fig. 3 with the CFL. For each dose point the nanodot is irradiated, kept in the dark for 8 min, and then read. The broken line, linear response, is based on the response of the OSLD at 20 cGy.

TABLE II. Characteristics of nanodots that were irradiated with 1, 2, and 5 kGy. The 1 and 5 kGy were delivered with Co-60 and the 2 kGy was delivered with Ir-192. Parameters are for Eq. (1). Experimental details are given in the text and the legend of Fig. 13.

Nanodot	Preirradiation (kGy)	A (counts/cGy)	B	C (cGy^{-1})
219401	0	966	0.066	0.001 46
290419	0	920	0.128	0.001 53
08120G	0	912	0.075	0.001 65
151653	0	930	0.104	0.001 59
219401	1	2299	≈0	≈0
290419	1	2283	≈0	≈0
08120G	5	2179	≈0	≈0
151653	5	2223	≈0	≈0
24102F	2	2624	≈0	≈0
19832V	2	2517	≈0	≈0

Preirradiated OSLDs can be optically annealed with a response similar to that shown in Fig. 3. However, it is found that a regeneration of the luminescence occurs in the dark after full annealing as shown in Fig. 13. This dark regenerated luminescence signal is equivalent to less than 22 cGy and has a half time of approximately two days.

V. DISCUSSION

The dose response of OSLDs made from Al_2O_3:C is found to be quite complex and is altered with accumulated dose. An understanding and control of these phenomena are essential for use of OSLDs for accurate dosimetric measurements. The phenomena measured in this work can be explained within the framework of the energy level diagram in Fig. 1 and reactions 1–15.

Optical annealing is a depletion of IET^- by photoionization and charge recombination (reactions 13 and 14). The inability to fully eliminate the luminescence by optical annealing as shown in Fig. 3 is because in the dark after optical annealing is ended, before reading the OSLD, electrons from

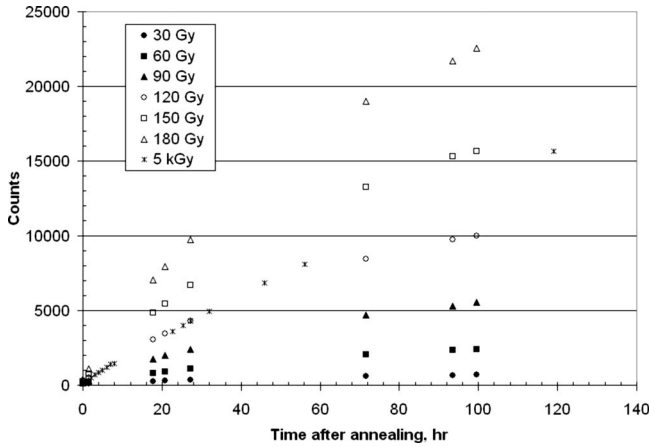

FIG. 13. Measurements of an OSLD signal after various times in the dark following optical annealing to the plateau value shown in Fig. 3 with the CFL. The various nanodots were irradiated with 30 to 180 Gy with 6 MV x rays and to 5 kGy with Co-60.

traps slightly deeper[17,18,37] than IET slowly lose their electrons. This regeneration of IET^- in the dark is easily seen in Fig. 13 and becomes more prominent with larger amounts of accumulated dose, which fills deep electron traps. The rise in counts in Fig. 13 corresponds to the regeneration of low concentrations of IET^-.

The use of a CFL for optical annealing is appealing since the apparatus is very inexpensive, there is little heat generated so melting of the plastic case of the OSLD is not a concern, large numbers of OSLDs can be annealed at the same time, and annealing overnight is adequate and requires no careful timing and intervention by a physicist. The THL anneals ten times more rapidly but the apparatus is more expensive and the method suffers from the disadvantages mentioned above.

The complex change in OSLD sensitivity and supralinearity shown in Figs. 4 and 7–10 are explained as a balance between DHT^+ and DET^-, which are stable at room temperature and cannot be photooxidized.[32,36] Supralinearity occurs because the concentrations of DET^- and deeper levels of IET^- increase with accumulated dose[12,32,36,38,42] and do not compete with IETs for radiation generated electrons (reactions 4 and 8). The magnitude of supralinearity, which can be gauged by the value of B, can increase and decrease with shifts in the equilibrium of deeper levels of IET^- concentration as seen in Fig. 8.

The decrease in OSLD sensitivity (counts/dose) with accumulated dose, shown in Fig. 7, has been reported previously.[12,13] This is due to the build up of DHT^+ (reaction 12), which competes with F^+ (reaction 14) for the optically stimulated electrons (reaction 13). The eventual increase in OSLD sensitivity above 60 Gy of accumulated dose, as seen in Figs. 7 and 10 is due to saturation of DHT^+ and continued increase in DET^- concentration. Extreme values of accumulated dose, greater than 1 kGy, result in high OSLD sensitivity and loss of supralinearity. In this condition, DHT^+ and DET^- concentrations have been saturated and optical annealing and irradiation are shifting the equilibrium of charges as follows:

$$F + \mathrm{IET} \underset{\text{optical annealing}}{\overset{\text{irradiation}}{\leftrightarrow}} F^+ + \mathrm{IET}^- \overset{\text{reading}}{\rightarrow} F + \mathrm{IET} + \text{luminescence},$$

where the reading only depletes the IET^- concentration by 0.05%.[12]

For the OSLDs with accumulated dose of greater than 1 kGy, the device response to dose becomes linear (Fig. 12). These devices are very easy to use. They are annealed immediately before use to remove any buildup of signal that occurs during storage in dark (Fig. 13). A calibration dose (Dcal) is delivered and after an 8 min wait, the signal (CNTcal) is read. The device is then placed on the patient, irradiated, and after an 8 min wait, the signal (CNTmeas) is read. The dose at the measurement position (Dmeas) on the patient is calculated as follows:

$$\mathrm{Dmeas} = \frac{\mathrm{Dcal}}{\mathrm{CNTcal}} \cdot \mathrm{CNTmeas} - \mathrm{Dcal}.$$

It is found that Dcal of 20 cGy is convenient for most clinical measurements.

The data in Table I indicate that new nanodots, when chosen at random from a batch obtained from the manufacturer, have quite different dose sensitivities as well as supralinear behavior. Based on these results, it is recommended that each OSLD be characterized even if they are from the same batch. The use of batch parameters, as suggested by Yukihara *et al.*,[23] is not supported by these data.

When an OSLD is given high dose without annealing (Fig. 11), the sensitivity increases with a plateau at about 40 Gy. In this case, DHT^+, deep levels of IET^-, and DET^- concentrations increase simultaneously. The sensitivity increase occurs because the DET^- and deeper levels of IET^- do not compete with IETs for radiation generated electrons (reactions 4 and 8).

VI. CONCLUSIONS

The use of OSLDs to make measurements with ±0.5% precision is possible if the complications described in this work are considered and controlled. The following guidelines should be followed:

1. OSLDs can be implemented in single-use protocol but they must be individually characterized.
2. OSLDs can be implemented in a multiple-use protocol but they must be characterized after each optical annealing since the OSLD characteristic change with accumulated dose.
3. OSLDs can be characterized by a quadratic equation model, which is useful over a range of 300 cGy.
4. OSLDs can be characterized by an exponential equation model, which is useful over a range of 1000 cGy.
5. OSLDs with an accumulated dose of greater than 1 kGy have a linear response to dose and in the dark have a regeneration of the luminescence signal with the half-life of approximately two days.

ACKNOWLEDGMENTS

The author would like to thank Landauer Co. for providing samples of nanodot dosimeters. No financial support was given to the author by the Landauer Co. The author would like to thank Dan Schmidt of Standard Imaging, Inc. for doing the Co-60 irradiations. Also, the author would like to thank Dr. Cliff Yahnke and Renu Sharma for many interesting technical discussions of this work.

[a]Electronic mail: pjursinic@wmcc.org

[1]International Commission on Radiation Units and Measurements, "Determination of absorbed dose in a patient irradiated by beams of x and gamma rays in radiotherapy procedures," ICRU Report No. 24, Bethesda, 1976.

[2]G. J. Kutcher *et al.*, "Comprehensive QA for radiation oncology: Report of AAPM radiation therapy committee Task Group 40," Med. Phys. **21**, 581–618 (1994).

[3]F. H. Attix, *Introduction to Radiological Physics and Radiation Dosime-*

try (Wiley, New York, 1986), Chap. 14, pp. 395–437.
[4]E. York, A. Rodica, L. Ding, D. Fontenla, A. Kalend, D. Kaurin, M. E. Masterson-McGary, G. Marinello, T. Matzen, A. Saini, J. Shi, W. Simon, T. Zhu, and X. R. Zhu, *Diode in vivo Dosimetry for Patients Receiving External Beam Radiation Therapy, Report of AAPM Task Group 62* (Medical Physics Publishing, Madison, 2005).
[5]S. Tavernier, A. Gektin, B. Grinyov, and W. W. Moses, *Radiation Detectors for Medical Applications* (Springer, Dordecht, 2005).
[6]M. S. Akselrod, V. S. Kortov, D. J. Kravetsky, and V. I. Gotlib, "High sensitivity thermoluminescent anion-defective α-Al_2O_3:C crystal detectors," Radiat. Prot. Dosim. **32**, 15–20 (1990).
[7]M. S. Akselrod, V. S. Kortov, and E. A. Goreleva, "Preparation and properties of α-Al_2O_3:C," Radiat. Prot. Dosim. **47**, 159–164 (1993).
[8]A. J. J. Bos, "High sensitivity thermoluminescence dosimetry," Nucl. Instrum. Methods Phys. Res. B **184**, 3–28 (2001).
[9]L. Bøtter-Jensen, N. Agersnap-Larsen, B. G. Markey, and S. W. S. McKeever, "Al_2O_3:C as a sensitive OSL dosimeter for rapid assessment of environmental photon dose rate," Radiat. Meas. **27**, 295–298 (1997).
[10]S. D. Miller and M. K. Murphy, "Technical performance of the Luxel α-Al_2O_3:C optically stimulated luminescence dosemeter element at radiation oncology and nuclear accident dose levels," Radiat. Prot. Dosim. **123**, 435–442 (2007).
[11]V. Schembri and B. J. M. Heijmen, "Optically stimulated luminescence (OSL) of carbon-doped aluminum oxide (AL_2O_3:C) for film dosimetry radiotherapy," Med. Phys. **34**, 2113–2118 (2007).
[12]P. A. Jursinic, "Characterization of optically stimulated luminescent dosimeters, OSLDs, for clinical dosimetric measurements," Med. Phys. **34**, 4594–4604 (2007).
[13]E. G. Yukihara and S. W. S. McKeever, "Optically stimulated luminescence (OSL) dosimetry in medicine," Phys. Med. Biol. **53**, R351–R379 (2008).
[14]S. W. S. McKeever, M. S. Akselrod, L. E. Colyott, N. Agersnap-Larsen, J. C. Polf, and V. Whitley, "Characteristics of Al_2O_3 for use in thermally and optically stimulated dosimetry," Radiat. Prot. Dosim. **84**, 163–168 (1999).
[15]R. C. Yoder and M. R. Salasky, "A dosimetry system based on delayed optically stimulated luminescence," Health Phys. **72**, S18–S19 (1997).
[16]M. S. Akselrod and S. W. S. McKeever, "A radiation dosimetry method using pulsed optically stimulated luminescence," Radiat. Prot. Dosim. **81**, 167–175 (1999).
[17]B. G. Markey, L. E. Colyott, and S. W. S. McKeever, "Time-resolved optically stimulated luminescence from α-Al_2O_3:C," Radiat. Meas. **24**, 457–463 (1995).
[18]L. Bøtter-Jensen and S. W. S. McKeever, "Optically stimulated luminescence dosimetry using natural and synthetic materials," Radiat. Prot. Dosim. **65**, 273–280 (1996).
[19]P. Allen and S. W. S. McKeever, "Studies of PTTL and OSL in TLD-400," Radiat. Prot. Dosim. **33**, 19–22 (1990).
[20]R. Gaza, S. W. S. McKeveer, and M. S. Akselrod, "Near-real time radiotherapy dosimetry using optically stimulated luminescence of Al_2O_3:C: Mathematical models and preliminary results," Med. Phys. **32**, 1094–1102 (2005).
[21]S. W. S. McKeever, M. S. Akselrod, and B. G. Markey, "Pulsed optically stimulated luminescence dosimetry using α-Al_2O_3:C," Radiat. Prot. Dosim. **65**, 267–272 (1996).
[22]S. W. S. McKeever and M. S. Akselrod, "Radiation dosimetry using pulsed optically stimulated luminescence of using α-Al_2O_3:C," Radiat. Prot. Dosim. **84**, 317–320 (1999).
[23]E. G. Yukihara, G. Mardirossian, M. Mirzasadeghi, S. Guduru, and S. Ahmad, "Evaluation of Al_2O_3:C optically stimulated luminescence (OSL) dosimeters for passive dosimetry of high-energy photon and electron beams in radiotherapy," Med. Phys. **35**, 260–269 (2008).
[24]C. S. Reft, "The energy dependence and dose response of a commercial optically stimulated luminescent detector for kilovoltage photon, megavoltage photon, and electron, proton, and carbon beams," Med. Phys. **36**, 1690–1699 (2009).
[25]M. S. Akselrod, L. Bøtter-Jensen, and S. W. S. McKeever, "Optically stimulated luminescence and its use in medical dosimetry," Radiat. Meas. **41**, S78–S99 (2006).
[26]J. M. Edmund and C. E. Andersen, "Temperature dependence of Al_2O_3:C response in medical luminescence dosimetry," Radiat. Meas. **42**, 177–189 (2007).
[27]M. C. Aznar, C. E. Andersen, L. Bøtter-Jensen, S. Å. J. Bäck, S. Mattsson, F. Kjaer-Kristoffersen, and J. Medin, "Real-time optical-fiber luminescence dosimetry for radiotherapy: Physical characteristics and application to photon beams," Phys. Med. Biol. **49**, 1655–1669 (2004).
[28]R. Gaza, S. W. S. McKeveer, M. S. Akselrod, A. Akselrod, T. Underwood, C. Yoder, C. E. Andersen, M. C. Aznar, C. J. Marckmann, and L. Bøtter-Jensen, "A fiber dosimetry method based on OSL from Al_2O_3:C: For radiotherapy applications," Radiat. Meas. **38**, 809–812 (2004).
[29]J. C. Polf, E. G. Yukihara, M. S. Akselrod, and S. W. S. McKeever, "Real-time luminescence from Al_2O_3:C fiber dosimeters," Radiat. Meas. **38**, 227–240 (2004).
[30]E. G. Yukihara, E. M. Yosimura, T. D. Lindstrom, S. Ahmad, K. K. Taylor, and G. Mardirossian, "High-precision dosimetry for radiotherapy using optically stimulated luminescence technique and thin Al_2O_3:C dosimeters," Phys. Med. Biol. **50**, 5619–5628 (2005).
[31]C. E. Andersen, M. C. Aznar, L. Bøtter-Jensen, S. Å. J. Bäck, S. Mattsson, and J. Medin, "Development of optical fibre luminescence techniques for real-time in-vivo dosimetry in radiatherapy," IAEA-CN-96–118, International Symposium on Standards and Codes of Practice in Medical Radiation Dosimetry, Vienna, Austria, 2002 (unpublished).
[32]E. G. Yukihara, V. H. Whitley, J. C. Polf, D. M. Klein, S. W. S. McKeever, A. E. Akselrod, and M. S. Alselrod, "The effects of deep trap population on the thermoluminescence of Al_2O_3:C," Radiat. Meas. **37**, 627–638 (2003).
[33]S. W. S. McKeever, N. L. Agersnap, L. Bøtter-Jensen, and V. Medjhal, "OSLD sensitivity changes during single aliquot procedures: Computer simulations," Radiat. Meas. **27**, 75–82 (1997).
[34]S. W. S. McKeever, "Optically stimulated luminescence dosimetry," Nucl. Instrum. Methods Phys. Res. B **184**, 29–54 (2001).
[35]M. L. Chithambo, "Concerning secondary thermoluminescence peaks in α-Al_2O_3:C," S. Afr. J. Sci. **100**, 524–527 (2004).
[36]M. S. Akselrod and E. A. Gorelova, "Deep traps in highly sensitive α-Al_2O_3:C TLD crystals," Nucl. Tracks Radiat. Meas. **21**, 143–146 (1993).
[37]H. Von Whitley and S. W. S. McKeever, "Photoionization of deep centers in Al_2O_3:C," Appl. Phys. (Berlin) **87**, 249–256 (2000).
[38]J. M. Edmund, C. E. Andersen, C. J. Marckmann, M. C. Aznar, M. S. Akselrod, and L. Bøtter-Jensen, "CW-OSL measurement protocols using optical fibre Al_2O_3:C dosimeters," Radiat. Prot. Dosim. **119**, 368–374 (2006).
[39]E. G. Yukihara, R. Gaza, S. W. S. McKeever, and C. G. Soares, "Optically stimulated luminescence and thermoluminescence efficiencies for high-energy heavy charged particle irradiation," Radiat. Meas. **38**, 59–70 (2004).
[40]F. D. Walker, L. E. Colyott, N. Agersnap-Larsen, and S. W. S. McKeever, "The wavelength dependence of light-induced fading of thermoluminescence from α-Al_2O_3:C," Radiat. Meas. **26**, 711–718 (1996).
[41]M. S. Akselrod, N. Agersnap-Larsen, V. Whitley, and S. W. S. McKeever, "Thermal quenching of F-center luminescence in Al_2O_3:C," J. Appl. Phys. **84**, 3364–3373 (1998).
[42]E. G. Yukihara, V. H. Whitley, S. W. S. McKeever, A. E. Akselrod, and M. S. Akselrod, "Effects of high-dose irradiation on the optically stimulated luminescence of Al_2O_3:C," Radiat. Meas. **38**, 317–330 (2004).
[43]P. R. Almond, P. J. Biggs, B. M. Coursey, W. F. Hanson, M. S. Huq, R. Nath, and D. W. O. Rogers, "AAPM's TG-51 protocol for clinical reference dosimetry of high-energy photon and electron beams," Med. Phys. **26**, 1847–1870 (1999).
[44]R. Nath, L. L. Anderson, G. Luxton, K. A. Weaver, J. F. Williamson, and A. S. Meigooni, "Dosimetry of interstitial brachytherapy sources: Recommendations of the AAPM radiation therapy committee Task Group No. 43," Med. Phys. **22**, 209–234 (1995).
[45]A Microsoft Excel spreadsheet is available from the author for doing this calculation.